Numerical multi-loop integration on heterogeneous many-core processors

E. de Doncker[1], A. Almulihi[1], F. Yuasa[2], N. Nakasato[3], H. Daisaka [4], T. Ishikawa [2]

[1]Dept. of Computer Science, W. Michigan Univ., U.S.A.

[2]High Energy Accelerator Research Organization (KEK), Tsukuba, Japan

[3]University of Aizu, Japan

[4]Hitotsubashi University, Japan

March 11, 2019

Outline

Outline

Outline

Outline

Outline

Outline

Loop integral - Introduction

- Higher order corrections are required for accurate theoretical predictions of the cross-section for particle interactions. Loop diagrams are taken into account, leading to the evaluation of loop integrals – for which analytic integration is not generally possible.
- The goal is to perform accurate loop integral computations; and to develop computer programs which evaluate multi-loop Feynman integrals numerically/directly.
- Previously in [7, 10, 6], we reported precise numerical results for 2-, 3- and 4-loop Feynman integrals using adaptive multi-dimensional integration and linear extrapolation. In [4, 5] we handle 2- and 3-loop integrals with (transformed) lattice rules on GPUs.
- Here we use composite lattice rules (with transformation) for 3- and 4-loop integrals, and parallel execution on systems with GPU or PEZY accelerators.

Loop integral - Representation

L-loop integral with N internal lines

$$\mathcal{F} = \frac{\Gamma\left(N - \frac{\nu L}{2}\right)}{(4\pi)^{\nu L/2}} (-1)^N \int_0^1 \prod_{r=1}^{N} dx_r \, \delta(1 - \sum x_r) \frac{C^{N-\nu(L+1)/2}}{(D - i\varrho C)^{N-\nu L/2}}$$

C and D are polynomials determined by the topology of the corresponding diagram and physical parameters; ν is the space-time dimension (i.e., = 4 unless used for regularization); $\varrho = 0$ unless D vanishes in the domain.

Number-theoretic methods MC, QMC

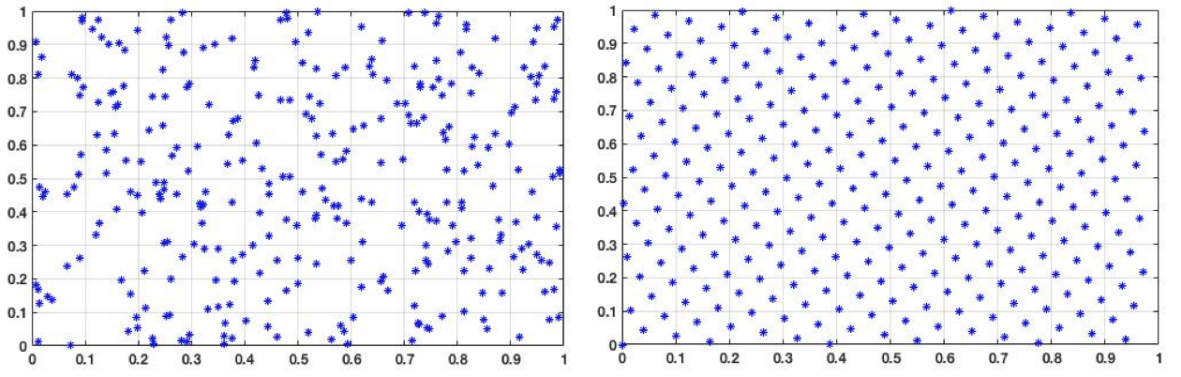

Figure: [MC-QMC] (left) 300 random points; (right) 300 points of 2-dimensional lattice constructed with generator vector z = (1, 129) [1]

Monte Carlo (MC): $\mathcal{I} = \int_{\mathcal{C}_d} f(\mathbf{x})\, d\mathbf{x} \;\approx\; Qf = \frac{1}{n}\sum_{j=0}^{n-1} f(\mathbf{x_j})$
where $\mathbf{x_j}$ are uniform random, and the error $|Qf - \mathcal{I}| \sim \mathcal{O}(1/\sqrt{n})$ as $n \to \infty$

Quasi-Monte Carlo (QMC), equidistributed rules, e.g., (good) lattice rules [3, 20]: the points $\mathbf{x_j}$ are generated on a (good) lattice in the half-open cube $\mathcal{U}_d = [0,1)^d$; with favorable convergence properties (compared to MC), particularly for smooth, 1-periodic

Lattice rules

Extension of 1D rectangle rule: $Rf = \frac{1}{n}\sum_{j=0}^{n-1} f(\frac{j}{n})$

Rank-1 lattice rule: $Q(\mathbf{z}, n)f = \frac{1}{n}\sum_{j=0}^{n-1} f(\{\frac{j}{n}\mathbf{z}\})$

where $\mathbf{z}$ is an integer generator vector with components
$z \in \mathcal{Z}_n = \{1 \leq z < n,\ gcd(z, n) = 1\}$;

$\{\mathbf{x}\}$ denotes the vector in $\mathcal{U}_d$ obtained by taking the fractional part of each component of $\mathbf{x}$;
classically n is prime (i.e., $\mathcal{Z}_n = \{1, 2, \ldots, n-1\}$)
(has been relaxed, cf. [12, 14])

Sample generators

100M, 7D: (1, 41883906, 22682973, 44229424, 29466837, 15518263, 42112409),
100M, 10D: (1, 41883906, 22682973, 44229424, 29466837, 8176047, 49462874, 1162485, 46871525, 36107330),
200M, 7D: (1, 76384079, 93229505, 12830863, 56635299, 54395013, 90891159)
400M, 7D: (1, 155987582, 55105452, 187223455, 109010593, 87245157, 73239020)
400M, 8D: (1, 155987582, 55105452, 187223455, 109010593, 87245157, 122592441, 131361432)
(100M denotes 100,000,007; 200M denotes 200000033; 400M denotes 400,000,009)
Note that projections of higher-dimensional generators can be used in lower dimensions.

We pre-compute the generators $(z_1, \ldots, z_d)$ using the component by component (CBC) algorithm by Nuyens and Cools [13, 14]. The CBC algorithm runs in $\mathcal{O}(d\, n \log(n))$ time and $\mathcal{O}(n)$ space.

Composite/embedded lattice rules

An embedded sequence is given in [20]; with m copies in r coordinate directions:

$$Q_r f = \frac{1}{m^r n} \sum_{k_r=0}^{m-1} \cdots \sum_{k_1=0}^{m-1} \sum_{j=0}^{n-1} f\left(\{\frac{j}{n}\mathbf{z} + \frac{1}{n}(k_1, \ldots, k_r, 0, \ldots, 0)\}\right)$$

for $0 \leq r \leq d$, n and m relatively prime, and $\mathbf{z}$ is a generator vector.

The points of Q_{r+1} include the points of Q_r for $0 \leq r < d$.
Q_r has $m^r n$ points and is of rank r for $1 \leq r \leq d$; Q_0 is of rank 1.
Q_d is the m^d-copy rule.

An error estimate is calculated for Q_d.

Composite/embedded lattice rules - Illustration

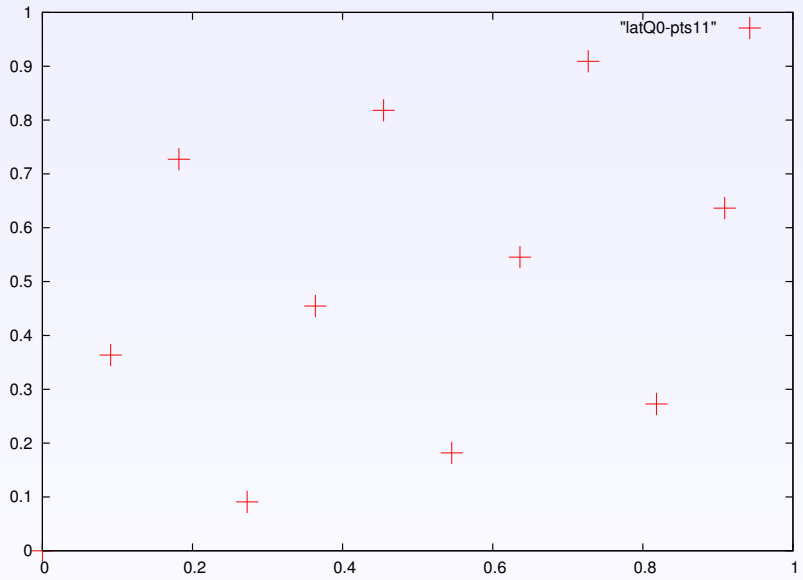

Figure: [2D rule Q_0] with 11 points, $\mathbf{z} = (1, 4)$

Composite/embedded lattice rules - Illustration

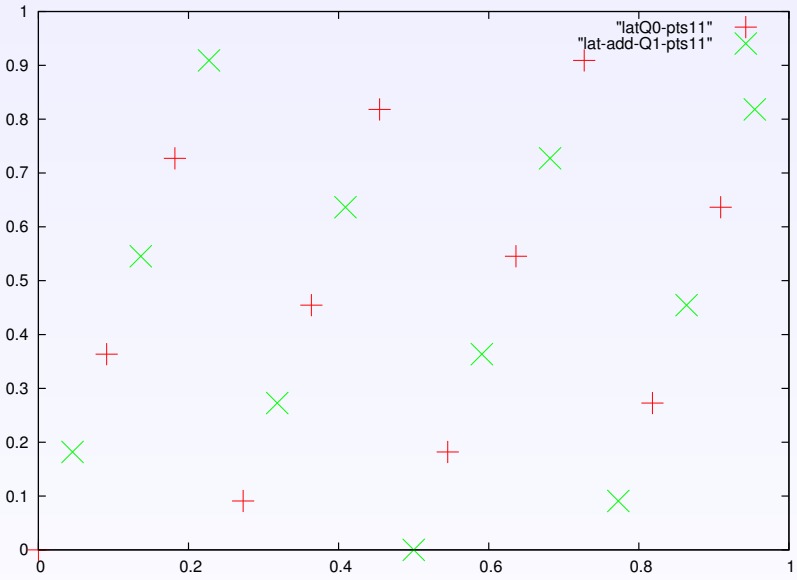

Figure: [2D rule Q_1] corresponding to Q_0, $\mathbf{z} = (1, 4)$

Q_1 includes the points of Q_0.

Composite/embedded lattice rules - Illustration

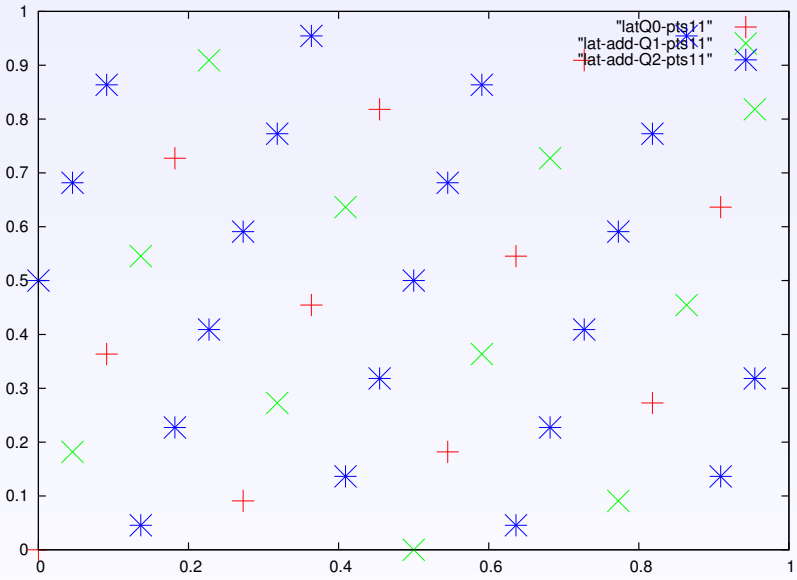

Figure: [2D rule Q_2] corresponding to Q_0, $\mathbf{z} = (1, 4)$

Q_2 includes the points of Q_0 and Q_1 (embedded sequence), and is the "2^2-copy" of Q_0.

Periodizing transformations

The lattice rule is applied after a periodizing transformation of the integrand. We have used transformations (tanh [17], $\sin^m$ [18, 19] that also smoothen singular behavior at the bounderies of the integration domain [4, 5].

Sidi $\sin^m$ transformations for an integral $\mathcal{I}f = \int_0^1 f(x)\,dx$:

$x = \Psi_m(t) = \frac{\theta_m(t)}{\theta_m(1)}, \quad m = 1, 2, \ldots$

with $\theta_m(t) = \int_0^t \sin^m(\pi u)\,du$.

$$\Psi_2(t) = t - \sin(2\pi t)/(2\pi), \quad \Psi_2'(t) = 2\sin^2(\pi t)$$
$$\Psi_4(t) = t + (-8\sin(2\pi t) + \sin(4\pi t))/(12\pi), \quad \Psi_4'(t) = \tfrac{8}{3}\sin^4(\pi t)$$
$$\Psi_6(t) = t - (45\sin(2\pi t) - 9\sin(4\pi t) + \sin(6\pi t))/(60\pi), \quad \Psi_6'(t) = \tfrac{16}{5}\sin^6(\pi t)$$

$\sin^m$ transformation (illustration)

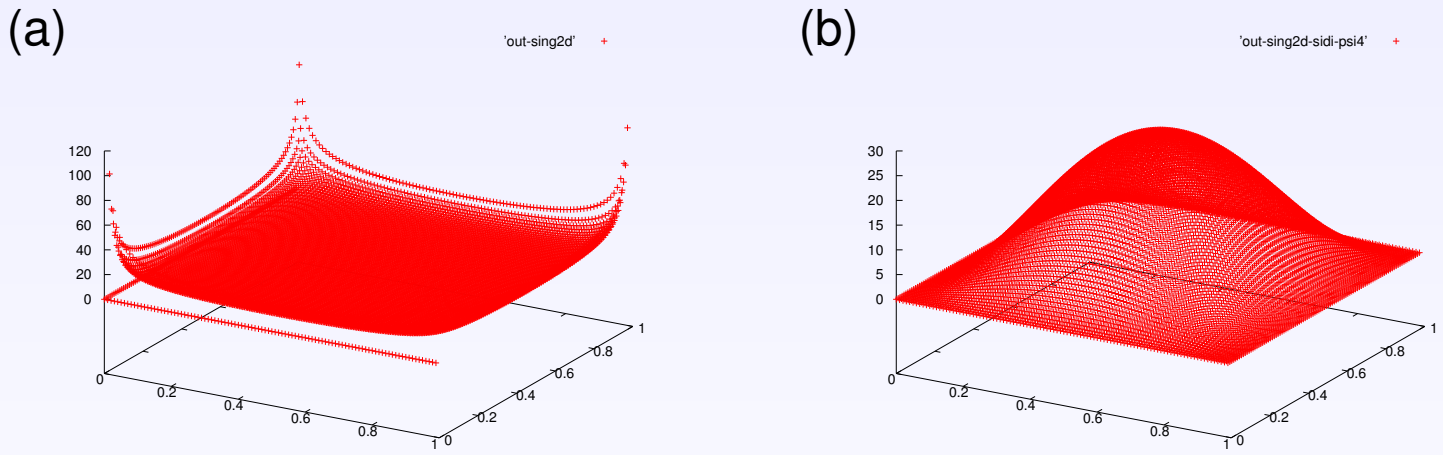

Figure: Ψ_4 transformation of $1/\sqrt{x_1 x_2 (1-x_1)(1-x_2)}$ over unit square: (a) without; (b) with transformation [4]

Sample 3-loop self-energy diagrams

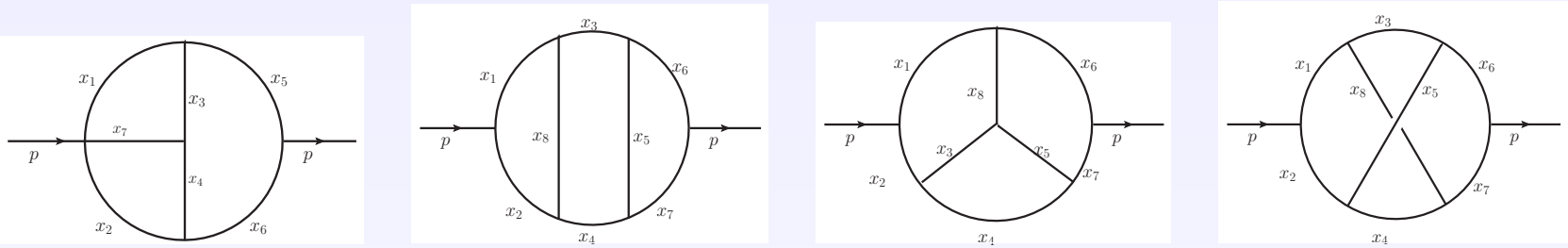

(a) (b) (c) (d)

Figure: [3ls] Sample 3-loop self-energy diagrams, cf. Laporta [11] (Diag. (r, t, u, v) with masses), Baikov and Chetyrkin [2] (Diag. (L_2, N_0, L_0) massless): (a) Diagram (r/N_2) $N = 7$; (b) Diagram (t/N_0) $N = 8$; (c) Diagram (u) $N = 8$; (d) Diagram (v/L_0) $N = 8$

Sample 4-loop self-energy diagrams

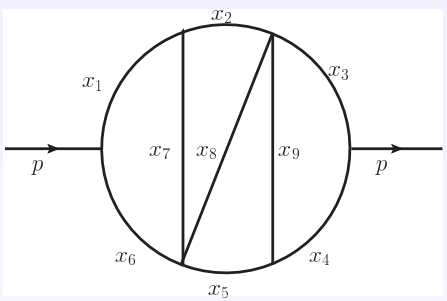

(a)

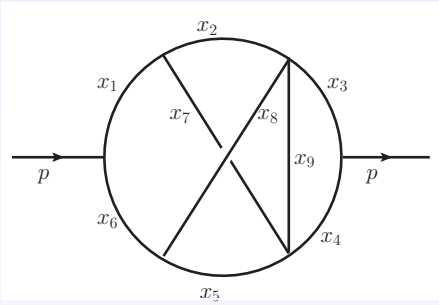

(b)

Figure: [4ls] 4-loop self-energy diagrams with massless internal lines, cf., Baikov and Chetyrkin [2]: (a) Diagram *M44*, $N = 9$; (b) Diagram *M45*, $N = 9$

GPU

GPU: Kepler 20m
From DeviceQuery program (NVIDIA), run on a node of thor.cs.wmich.edu :

CUDA Capability Major/Minor version number:	3.5
Total amount of global memory:	4800 MBytes (5032706048 bytes)
(13) Multiprocessors x (192) CUDA Cores/MP:	2496 CUDA Cores
GPU Clock rate:	706 MHz (0.71 GHz)
Memory Clock rate:	2600 Mhz
Memory Bus Width:	320-bit
L2 Cache Size:	1310720 bytes
Total amount of constant memory:	65536 bytes
Total amount of shared memory per block:	49152 bytes
Total number of registers available per block:	5536
Warp size:	32
Maximum number of threads per multiprocessor:	2048
Maximum number of threads per block:	1024
Integrated GPU sharing Host Memory:	No
Support host page-locked memory mapping:	Yes
Device has ECC support:	Enable
Device supports Unified Addressing (UVA):	Yes

Suiren2 (ZettaScaler 2.2)

Figure: Suiren2 at KEK, liquid immersion cooling, many-core supercomputer

Suiren2 (ZettaScaler 2.2)

From top500.org:
Suiren2 - ZettaScaler-2.2, Xeon D-1571 16C 1.3GHz, Infiniband EDR

Site	High Energy Accelerator Research Organization /KEK
System URL:	http://www.exascaler.co.jp/
Manufacturer:	PEZY Computing / Exascaler Inc.
Cores:	762,624
Memory:	26,112 GB
Processor:	Xeon D-1571 16C 1.3GHz
Interconnect:	Infiniband EDR
Linpack Performance	Rmax: 797.994 TFlop/s; Nmax: 1,238,016
Theoretical Peak	Rpeak: 1,082.57 TFlop/s
Power Consumption	Power: 47.40 kW (Submitted)

Configuration at KEK:
- 6 tanks
- 2 bricks (high density server boards) per tank
- total bricks is $6 \times 2 = 12$
- 4 nodes per brick, 8 PEZY-SC2 boards per node
- total $8 \times 4 = 32$ PEZY-SC2 accelerator boards per brick
- total number of nodes: $4 \times 12 = 48$
- total number of PEZY-SC2 boards: $48 \times 8 = 384$

Suiren2 (ZettaScaler 2.2)

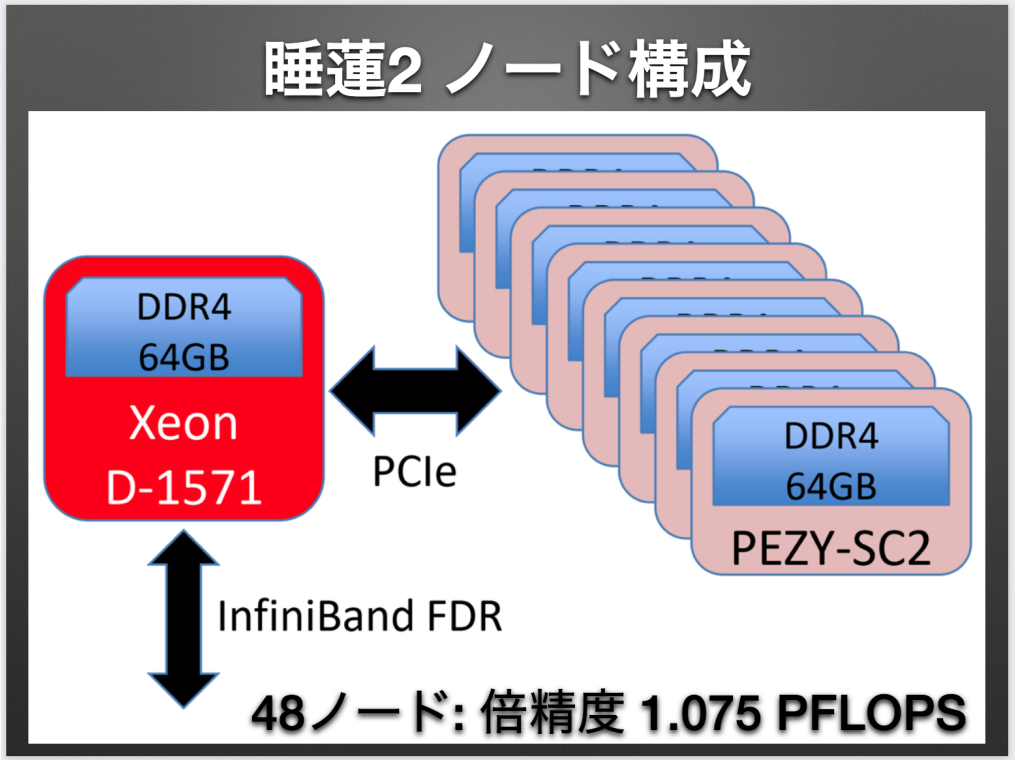

Figure: Suiren2 node configuration

PEZY-SC2

MIMD manycore PEZY-SC2 processor [21]
Some specifications:

Frequency	1GHz
Cache Memory (Chip Total)	L1:4MB(D), 8MB(I) L2: 8MB(D), 4MB(I) LLC: 40MB
Local Memory	Total 40MB (20KB/PE)
PE	2,048 (1986) core 2issue/cycle 8 way time-sliced fine-grain multi-threading (Total: 16,384 threads)
Peak Performance	8.2TFLOPS(SP), 4.1TFLOPS(DP), 16.4TFLOPS(HP)
Power	180W (Peak Estimated)

Programming model [21]

- PZCL environment: program consists of a CPU (host) program in C++ and kernel in OpenCL
- CPU code: sets up kernel code and buffers, initializes buffers allocated in PEZY-SC2, and invokes kernel code on PEZY-SC2 as multiple threads
- threads can run independently on MIMD PEZY-SC2 processor
- program can be generated by Goose compiler [8, 9]
- Goose uses compiler directives (pragmas) similar to OpenMP [16] and OpenACC [15]

(Simple) LR integration for 3-loop massive self-energy diagrams on GPU

DIAGRAM	N	# POINTS n	RESULT	ERROR	TIME [s]
Fig [3ls] (r)	7	200M	1.34139904258	1.99 e-07	0.616
		350M	1.34139953791	2.96 e-07	1.080
		Exact:	1.34139924145		
Fig [3ls] (t)	8	200M	0.27960944661	5.23 e-07	0.749
		350M	0.27960937820	4.55 e-07	1.314
		Exact:	0.27960892328		
Fig [3ls] (u)	8	200M	0.18262710188	1.36 e-07	0.752
		350M	0.18262769916	4.62 e-07	1.317
		Exact:	0.18262723754		
Fig [3ls] (v)	8	200M	0.14801298928	3.15 e-07	0.740
		350M	0.14801307409	2.30 e-07	1.299
		Exact:	0.14801330396		

Table: (Simple) LR integration for 3-loop massive self-energy diagrams on GPU [4, 5]

$(m = 1, 2)$ LR results for 3-loop massive self-energy diagrams on GPU

DIAGRAM	N	# PTS n	m	RESULT	ABS.ERR.	TIME [s]
Fig [3ls] (t)	8	400M	1	0.2796089827126	5.94 e-08	0.999
			2	0.2796089232826	2.52 e-14	127.8
		5^{13} $(7D)$	1	0.2796089226167	6.66 e-10	3.047
			2	0.2796089232824	1.63 e-13	390.1
Exact:				0.2796089232826		
Fig [3ls] (u)	8	400M	1	0.1826272683315	3.08 e-08	1.001
			2	0.1826272375394	2.18 e-13	128.1
		5^{13} $(7D)$	1	0.1826272372834	2.56 e-10	3.054
			2	0.1826272375391	1.46 e-13	391.0
Exact:				0.1826272375392		
Fig [3ls] (v)	8	400M	1	0.1480133458323	4.19 e-08	1.558
			2	0.1480133039588	2.37 e-13	199.4
		5^{13} $(7D)$	1	0.1480133033037	6.55 e-10	4.752
			2	0.1480133039581	3.46 e-13	608.1
		$(15 \rightarrow 7D)$	1	0.1480133034035	5.55 e-10	4.751
			2	0.1480133039583	8.97 e-14	608.6
Exact:				0.1480133039584		

Table: $(m = 1, 2)$ LR results for 3-loop massive self-energy diagrams on GPU

$(m = 1, 2)$ LR results for 4-loop massless self-energy diagrams on GPU

DIAGRAM	N	# PTS n	m	RESULT	ABS.ERR.	REL.ERR.	TIME [s]
Fig [4ls] (*M44*)	9	100M	1	55.657754	7.25 e-02	1.30 e-03	0.430
			2	55.586092	8.38 e-04	1.51 e-05	113.4
		400M	1	55.600351	1.51 e-02	2.72 e-03	1.770
			2	55.585416	1.62 e-04	2.91 e-06	452.9
		5^{13} $(15 \rightarrow 8D)$	1	55.577700	7.55 e-03	1.36 e-04	5.400
			2	55.585135	1.19 e-04	2.14 e-06	1382
Exact:				55.585254			
Fig [4ls] (*M45*)	9	100M	1	52.058688	4.08 e-02	7.85 e-04	0.450
			2	52.018436	5.67 e-04	1.09 e-05	114.9
		400M	1	52.014437	1.43 e-03	6.96 e-05	1.794
			2	52.017790	7.92 e-05	1.52 e-06	459.4
		5^{13} $(15 \rightarrow 8D)$	1	52.012072	5.80 e-03	1.11 e-04	5.474
			2	52.017807	6.17 e-05	1.19 e-06	1402
Exact:				52.017869			

Table: $(m = 1, 2)$ LR results for 4-loop massless self-energy diagrams on GPU

$(m = 2)$ 400M pts. LR results for 3-loop massive self-energy diagram (u) on Suiren2

DIAGRAM	N	#PTS. n	TIMES [S] ON SUIREN2, NXTY: X NODES, Y TASKS			
			1 node	2 nodes	4 nodes	8 nodes
Fig [3ls] (u)	8	400M	n1t1: 140.8			
			n1t2: 71.55	n2t1: 73.73		
			n1t4: 36.71	n2t2: 37.04	n4t1: 36.64	
			n1t8: 19.21	n2t4: 18.97	n4t2: 18.89	n8t1: 18.76
				n2t8: 10.01	n4t4: 9.913	n8t2: 9.839
					n4t8: 5.681	n8t4: 5.470
						n8t8: 3.475

Table: $(m = 2)$ 400M results for 3-loop massive self-energy diagram (u) on Suiren2; Abs. err. = 4.28e-11; Loop blocks of size $128 * 32$; Compare to GPU: 128.1 s

$(m = 2)$ 5^{13} pts. LR results for 3-loop massive self-energy diagram (u) on Suiren2

DIAGRAM	N	#PTS. n	TIMES [S] ON SUIREN2, NXTY: X NODES, Y TASKS			
			1 node	2 nodes	4 nodes	8 nodes
Fig [3ls] (u)	8	5^{13}	n1t1: 433.4			
			n1t2: 219.8	n2t1: 218.4		
			n1t4: 112.0	n2t2: 110.3	n4t1: 112.1	
			n1t8: 57.73	n2t4: 56.72	n4t2: 56.66	n8t1: 56.33
				n2t8: 30.14	n4t4: 29.74	n8t2: 29.05
					n4t8: 16.74	n8t4: 15.90
						n8t8: 9.899

Table: $(m = 2)$ 5^{13} pts. $(7D)$ results for 3-loop massive self-energy diagram (u) on Suiren2; Abs. err. = 4.24e-11; Loop blocks of size $128 * 32$; Compare to GPU: 391.0 s

($m = 2$) 400M pts. LR results for 3-loop massless self-energy diagram L_0 on Suiren2

Diagram	N	#Pts. n	Times [s] on Suiren2, nXtY: X nodes, Y tasks			
			1 node	2 nodes	4 nodes	8 nodes
Fig [3ls] (t)	8	400M	n1t1: 143.0			
			n1t2: 71.53	n2t1: 71.52		
			n1t4: 36.66	n2t2: 36.61	n4t1: 36.58	
			n1t8: 19.01	n2t4: 18.92	n4t2: 18.87	n8t1: 18.72
				n2t8: 10.09	n4t4: 9.860	n8t2: 9.846
					n4t8: 5.674	n8t4: 5.456
						n8t8: 3.471

Table: ($m = 2$) 400M results for 3-loop massless self-energy diagram L_0 on Suiren2; Abs. err. = 8.98e-07, Rel. err. = 4.33e-08; Loop blocks of size $128 * 32$; Compare to GPU: 128.0 s

$(m = 2)$ 5^{13} pts. LR results for 3-loop massless self-energy diagram L_0 on Suiren2

DIAGRAM	N	#PTS. n	TIMES [S] ON SUIREN2, NXTY: X NODES, Y TASKS			
			1 node	2 nodes	4 nodes	8 nodes
Fig [3ls] (t)	8	5^{13}	n1t1: 432.7			
			n1t2: 217.8	n2t1: 217.7		
			n1t4: 111.7	n2t2: 111.4	n4t1: 112.0	
			n1t8: 58.33	n2t4: 57.58	n4t2: 56.58	n8t1: 56.23
				n2t8: 30.68	n4t4: 29.70	n8t2: 29.01
					n4t8: 16.70	n8t4: 15.91
						n8t8: 9.857

Table: $(m = 2)$ 5^{13} pts. $(7D)$ results for 3-loop massless self-ene rgy diagram L_0 on Suiren2; Abs. err. = 1.71e-07, Rel. err. = 8.22e-09; Loop blocks of size $128 * 32$;
Compare to GPU: 390.6 s

$(m = 2)$ LR results for 4-loop massless self-energy diagram *M44* on Suiren2

DIAGRAM	N	#PTS. n	TIMES [S] ON SUIREN2, NXTY: X NODES, Y TASKS			
			1 node	2 nodes	4 nodes	8 nodes
Fig [4ls] *M45*	9	400M	n1t1: 332.5 n1t8: 43.32			
				n2t8: 22.36		
					n4t8: 11.90	
						n8t8: 6.711
Fig [4ls] *M45*	9	5^{13}				
				n2t8: 68.58		
					n4t8: 35.82	
						n8t8: 19.49

Table: $(m = 2)$ results for 4-loop massless self-energy diagram *M45* on Suiren2; Loop blocks of size $128 * 32$; 400M pts.: Abs. err. = 2.57e-05, Rel. err. = 4.94e-07, Compare to 400M pts. GPU time: 459.5 s; 5^{13} pts.: Abs. err. = 1.02e-06, Rel. err. = 1.95e-08, Compare to 5^{13} pts. GPU time: 1402 s

Conclusions

- A parallel composite/embedded lattice rule method is presented for the calculation of Feynman loop integrals, using a periodizing transformation that deals with singularities at the boundaries of the integration domain.
- The algorithm is implemented in CUDA C (for GPU accelerator). and in C++ with Goose (for PEZY Exascaler accelerator).
- Test results are given for classes of 3- and 4-loop self-energy loop diagrams, with or without masses, and using simple ($m = 1$) and composite ($m = 2$) lattice rules.
- The accuracy improves considerably from ($m = 1$) to ($m = 2$) and supersedes that of adaptive parallel integration with the ParInt package for these problems.
- The execution times are decreased considerably on the Exascalar system, using multiple PEZY accelerators per node and multiple nodes. The programs incorporate Goose and MPI, and run unchanged on different configurations.

Research support acknowledgments

- the Large Scale Computational Sciences with Heterogeneous Many-Core Computers, Grant-in-Aid for High Performance Computing with General Purpose Computers from MEXT (Ministry of Education, Culture, Sports, Science and Technology-Japan)
- National Science Foundation (NSF) under Award Number 1126438
- KEK
- WMU
- NVIDIA

Questions?

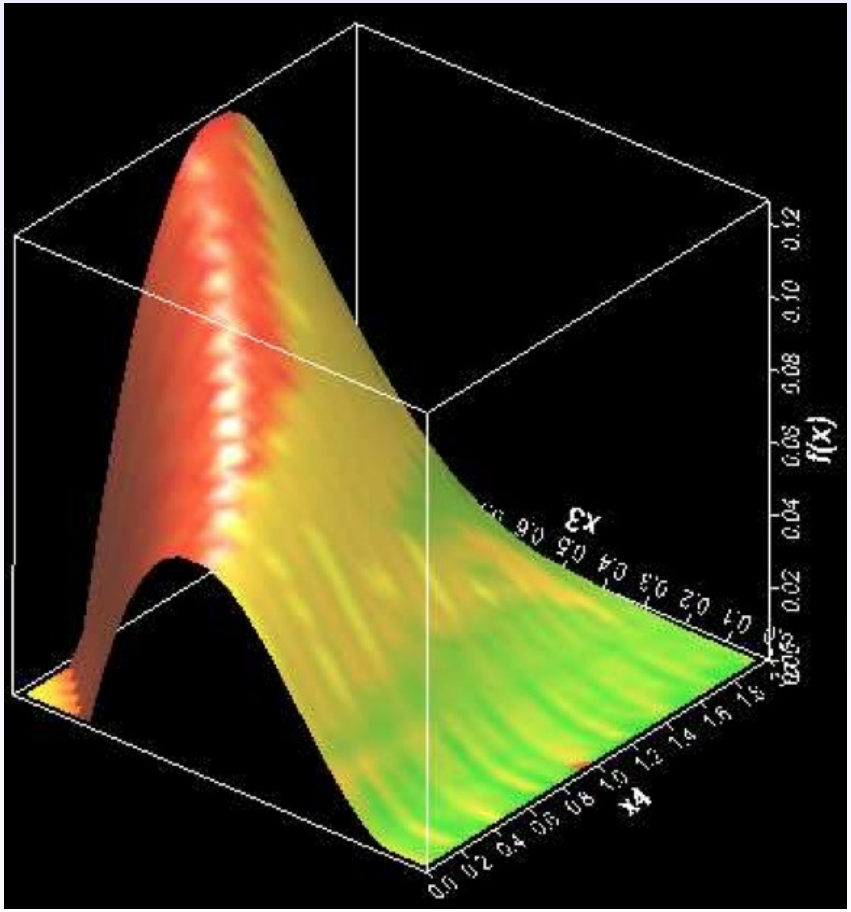
0.0 0.2 0.4 0.6 0.8 1.0 1.2 1.4 1.6 1.8
x4
0.0 0.2 0.4 0.6 0.8 1.0
x3
0.0 0.02 0.04 0.06 0.08 0.10 0.12
f(x)

Bibliography

Almulihi, A., and de Doncker, E.
Accelerating high-dimensional integration using lattice rules on GPUs.
In *Int. Conf. on Comput. Science and Comput. Intelligence (CSCI'17); IEEE Xplore; ISBN-13: 978-1-5386-2652-8; BMS Part # CFP1771X-USB; DOI 10.1109/CSCI.2017.313* (2017).
https://american-cse.org/csci2017.

Baikov, B. A., and Chetyrkin, K. G.
Four loop massless propagators: An algebraic evaluation of all master integrals.
Nuclear Physics B 837 (2010), 186–220.

Davis, P. J., and Rabinowitz, P.
Methods of Numerical Integration.
Academic Press, New York, 1975.

de Doncker, E., Almulihi, A., and Yuasa, F.
High speed evaluation of loop integrals using lattice rules.
Journal Phys.: Conf. Ser. (JPCS), IOP Series 1085, 052005 (2018).

http://iopscience.iop.org/article/10.1088/1742-6596/1085/5/052005.

DE DONCKER, E., ALMULIHI, A., AND YUASA, F.
Transformed lattice rules for Feynman loop integrals.
Journal Phys.: Conf. Ser. (JPCS), IOP Series 1136, 012002 (2018).
doi:10.1088/1742-6596/1136/1/012002.

DE DONCKER, E., FUJIMOTO, J., HAMAGUCHI, N., ISHIKAWA, T., KURIHARA, Y., SHIMIZU, Y., AND YUASA, F.
Quadpack computation of Feynman loop integrals.
Journal of Computational Science (JoCS) 3, 3 (2011), 102–112.
doi:10.1016/j.jocs.2011.06.003.

DE DONCKER, E., YUASA, F., KATO, K., ISHIKAWA, T., KAPENGA, J., AND OLAGBEMI, O.
Regularization with numerical extrapolation for finite and UV-divergent multi-loop integrals.
Computer Phys. Communications 224 (2018), 164–185.
https://doi.org/10.1016/j.cpc.2017.11.001.

GOOSE.
Goose software package user's guide - for goose version 1.3.3, 2010.
K & F Computing Research Co. (in English).

GOOSE.
Goose - GRAPE9-MPx - for goose version 1.5.0, 2014.
K & F Computing Research Co. (in Japanese).

KATO, K., DE DONCKER, E., ISHIKAWA, T., KAPENGA, J., OLAGBEMI, O., AND YUASA, F.
High performance and increased precision techniques for Feynman loop integrals.
Journal Physics: Conf. Ser. 762 (2016).
012070, iopscience.iop.org/article/10.1088/1742-6596/762/1/012070.

LAPORTA, S.
High-precision calculation of multi-loop Feynman integrals by difference equations.
Int. J. Mod. Phys. A 15 (2000), 5087–5159.
arXiv:hep-ph/0102033v1.

NIEDERREITER, H.
Existence of good lattice points in the sense of hlawka.
Monatshefte für Mathematik 86 (1978), 203–219.

NUYENS, D., AND COOLS, R.

Fast algorithms for component-by-component construction of rank-1 lattice rules in shift-invariant reproducing kernel Hilbert spaces.
Math. Comp. 75, 903-920 (2006).

NUYENS, D., AND COOLS, R.
Fast component-by-component construction of rank-1 lattice rules with a non-prime number of points.
Journal of Complexity 22, 4-28 (2006).

OPENACC.
http://www.openacc-standard.org.

OPENMP.
http://www.openmp.org.

SAG, T. W., AND SZEKERES, G.
Numerical evaluation of high-dimensional integrals.
Math. Comp. 18, 86 (1964), 245–253.

SIDI, A.
A new variable transformation for numerical integration.
International Series of Numerical Mathematics 112 (1993), 359–373.

SIDI, A.
Extension of a class of periodizing transformations for numerical integration.
Math. Comp. 75 (2006), 327–343.

SLOAN, I., AND JOE, S.
Lattice Methods for Multiple Integration.
Oxford University Press, Oxford, 1994.

TORII, S., AND ISHIKAWA, H.
ZettaScaler: Liquid immersion cooling manycore based supercomputer.
In *Keynote, CANDAR17, ExaScaler Inc. and PEZY Computing* (2017).
https://www.pezy.co.jp/wp-content/uploads/2019/02/Keynote_candar2017.pdf.